J Stat Phys (2011) 143: 148–167
DOI 10.1007/s10955-011-0171-5

Markov Properties of Electrical Discharge Current Fluctuations in Plasma

S. Kimiagar · M. Sadegh Movahed · S. Khorram · M. Reza Rahimi Tabar

Received: 6 June 2010 / Accepted: 2 March 2011 / Published online: 19 March 2011

Abstract Using the Markovian method, we study the stochastic nature of electrical discharge current fluctuations in the Helium plasma. Sinusoidal trends are extracted from the data set by the Fourier-Detrended Fluctuation analysis and consequently cleaned data is retrieved. We determine the Markov time scale of the detrended data set by using likelihood analysis. We also estimate the Kramers-Moyal's coefficients of the discharge current fluctuations and derive the corresponding Fokker-Planck equation. In addition, the obtained Langevin equation enables us to reconstruct discharge time series with similar statistical properties compared with the observed in the experiment. We also provide an exact decomposition of temporal correlation function by using Kramers-Moyal's coefficients. We show that for the stationary time series, the two point temporal correlation function has an exponential decaying behavior with a characteristic correlation time scale. Our results confirm that, there is no definite relation between correlation and Markov time scales. How-

S. Kimiagar
Department of Physics, Science Faculty, Tehran Central Branch, Islamic Azad University, Tehran, Iran
e-mail: kimia@khayam.ut.ac.ir

M. Sadegh Movahed (✉)
Department of Physics, Shahid Beheshti University, G.C., Evin, Tehran 19839, Iran
e-mail: m.s.movahed@ipm.ir

M. Sadegh Movahed
School of Astronomy, Institute for Research in Fundamental Sciences, (IPM), P.O. Box 19395-5531, Tehran, Iran

S. Khorram
Research Institute for Applied Physics and Astronomy, University of Tabriz, Tabriz 51664, Iran
e-mail: sirousk@yahoo.com

M. Reza Rahimi Tabar
Department of Physics, Sharif University of Technology, P.O. Box 11365-9161, Tehran, Iran

M. Reza Rahimi Tabar
Fachbereich Physik, Universität Osnabrück, Barbarastraße 7, 49076 Osnabrück, Germany
e-mail: mohammed.r.rahimi.tabar@uni-oldenburg.de

ever both of them behave as monotonic increasing function of discharge current intensity. Finally to complete our analysis, the multifractal behavior of reconstructed time series using its Keramers-Moyal's coefficients and original data set are investigated. Extended self similarity analysis demonstrates that fluctuations in our experimental setup deviates from Kolmogorov (K41) theory for fully developed turbulence regime.

Keywords Turbulence · Markov processes · Plasma fluctuations

1 Introduction

Many natural phenomena are identified by a degree of stochasticity. Turbulent flows, seismic recordings and plasma fluid are a few examples of such phenomena [1–28]. Interpretation and estimation of physical and chemical properties of plasma fluid have been one of the main research areas in the science of electromagnetic hydrodynamics. It is well-known that discharge current fluctuations in the plasma often exhibits irregular and complex behavior [27, 28]. Fluctuations happening commonly in the plasmas of gas discharges are responsible for a significant aliquot part of physical and chemical properties of plasma and reveal many interesting manner of plasma dynamics, energy carrier, neutrality and shielding areas form microscopic as well as macroscopic points of view. Generally, fluctuations arising in plasma can be classified as: fluctuations in the electron temperature, fluctuations in the local plasma space-potential which is assumed to be periodic and fluctuations in the local random electrical current in the plasma [2]. It is supposed that, these kinds of fluctuations can be characterized according to the following main properties. The statistics of time series are roughly homogeneous and isotropic, the spatial correlation length scale is shorter than the background charge density and temperature flow characteristic length scales. The autocorrelation function of such process is also demonstrated as anti-correlated behavior (see e.g. [6, 27, 28]). The phase space of relevant factors which influence the trajectory of current fluctuations measured by Langmuir probe in the plasma is enormously large. Therefore, there is no remedy to use stochastic tools for investigating their statistical properties. In the presence of complexity as well as non-linearity in a typical plasma fluctuations, traditional methods in data analysis encounter with spurious or at least give unreliable results for explanation of plasma dynamics.

It is impossible to consider all physical features of plasma fluctuations as a turbulent transport in the context of deterministic methods. Also finding a good agreement between properties of plasma discharge fluctuations and that of for a turbulence regime can play an important role to track the dissipation of energy transfer at different scale in the plasma fluid for various values of current intensity by means of multiplicative cascade model.

There are many stochastic analysis devoted to study the plasma fluctuations. Fluctuations of electric and magnetic fields of plasma, spectral density, logistic mapping and nonlinearity of ionization wave have been investigated in Refs. [2–6, 29–31]. For example, Carreras *et al.*, have demonstrated that plasma fluctuations behave as a multifractal process with nonlinearity comparable to the fluid turbulence [32]. Also Budaev *et al.*, [33, 34] by using the scaling behavior of structure function and wavelet transform modulus maxima (WTMM), showed that the anomalous transport of particles in the plasma has multifractal nature. The universality of stochastic properties of different plasma with various experimental equipments as well as different physical and chemical operating regimes, have also been explored in some previous studies. These universality which can be determined in experiment are led to insights through the understanding of plasma dynamics. Universality in power spectrum of plasma fluctuations for various plasma has been investigated in [35].

Although the analysis of fluctuations in plasma has a long history, there are, nevertheless, some important issues, such as stochastic features and most important characteristic time and length scales in the presence of nonstationarity and trends have remained unexplained so far. Recently a robust statistical method has been developed to explore an effective equation that can reproduce stochastic data with an accuracy comparable to the measured one [7–11, 36–40]. As in many early researches has been confirmed, one may utilize it to:

(1) reconstruct the original process with similar statistical properties, and
(2) understand the nature and properties of the stochastic process [7–24, 36]. One of a main task in the evolution of plasma fluctuations is to quantify most relevant statistical properties such as structure function, characteristic time and length scales, drift and diffusion coefficient. In addition, deriving a reliable stochastic model to reconstruct the data measured by Langmuir probe will be of interest in the simulation of plasma fluctuation.

Actually, data measured by Langmuir probe integrate fluctuations in plasma quantities such as number density of charge carriers, electron temperature, floating potential, heat transport and so on, consequently the statistical characteristics of probe fluctuations can be used to obtain information from physical and chemical points of view. For these purpose we use a robust methods in the complex systems namely, Markovian method to analyze the plasma fluctuations during steady state plasma discharge.

Due to the many limitations in an experimental setup for measuring desired fluctuations, the original fluctuations may be influenced by some trends and nonstationarities. In addition, the following necessary conditions should be satisfied to infer valuable statistical results:

(i) The length of measured fluctuations must be large enough.
(ii) The contribution of superimposed trends and nonstationarities on the recorded data must be small enough in comparison to intrinsic fluctuations or at least distinguishable.

Unfortunately in many cases of practical measurements, above necessary conditions cannot be specified. Identifying trends and foundation of proper detrending operations are important step toward robust analysis. Meanwhile, unfortunately, there is no unique definition of trend and any proper method for extracting it from underlying data sets in the presence of nonstationarities [41–46]. On the other hands, trend in a real world data series especially for non-stationary one, is an intrinsic function imposed by the nature on data set [47]. To recognize the trend on a data set, one can investigate the series in whole domain or on some specific span of domains. Singular value decomposition (SVD) as a filtering procedure has also been introduced to detrend of signals [48–50]. The other method for detrending is so-called Fourier Detrended Fluctuation Analysis (F-DFA). This method behaves like a high pass filter and useful for removing expected sinusoidal trends embedded in underlying data set.

In our previous study concerning plasma fluctuations [6], we found that the plasma fluctuations in the various discharge current intensities, behave as anti-correlated signals. For highly ionized fluid each large deviation from the electrostatic equilibrium is shielded by a cloud of oppositely-charged particles [51–54]. This also may be related to the fast dissipation of turbulent kinetic energy in plasma [34].

In this paper, we would like to extend our previous analysis and open a new insight to reconstruct the stochastic fluctuations and examine the turbulent feature of underlying data sets. The study of the universality, non-Gaussianity, multifractality and scaling behavior of structure function also will be other aims in this study. At first we should remove trends due to electronic instrumental systematic noises, alternative current oscillation and the fluctuations of striation areas near the anode and cathode plates. As discussed in details in [6],

we compute power spectrum of series using the method proposed in [46]. Now it is easy to track the influence of dominant sinusoidal trends represented as peaks in the spectral density versus frequency. By removing these coefficients, actually we diminish their contributions in the reconstruction of fluctuations. If this part has been done well, the crossovers in the fluctuations function given by multifractal detrended fluctuations analysis for reconstructed series will be disappeared and finally the cleaned data sets for further investigations will be retrieved. The minimum number of coefficients in the Fourier space should be eliminated to remove dominant sinusoidal trends is approximately 400. It is worth noting that to find cross-correlation between two different series Singular Value Decomposition could be used to guarantee the synchronization. Here using the Markovian method, we explore the statistical properties of detrended discharge current fluctuations. Then a Fokker-Planck evolution operator and Langevin equation will be found [7–11]. To complete our analysis we will investigate the multifractal exponent derived by Markovian method and compare it with that of computed by extended self similarity method. In addition, we discuss about the different sources of the multifractality in discharge current fluctuations.

The rest of this paper is organized as follows: In Sect. 2, we give an explanation of our experimental set up used for recording plasma fluctuations. Section 3 is devoted to a brief summary of the most important notions and theorems on Markovian method and their application to the analysis of empirical data. Using the likelihood statistics, we determined Markov time scale. Section 4 contains the main results of our analysis and estimate the Fokker-Planck and Langevin equations which govern the probability density function and stochastic variable (discharge current), respectively. An exact decomposition equation for computing temporal correlation function and distinguishing between Markov and correlation time scale are explained in detail in Sect. 4. Non-Gaussianity and multifractality nature of original and reconstructed time series are also given in Sect. 5. Section 6 closes with a discussion and conclusion of the present results.

2 Experimental Equipment

To explore the complex nature of the discharge current fluctuations in a typical plasma, we constructed an experimental setup as indicated in Fig. 1. The plasma chamber has two copper electrodes attached to the ends of discharge glass tube, 80 mm in diameter and 110 cm in length. One of these electrode is the anode (a flat copper plate as a positive pole), while

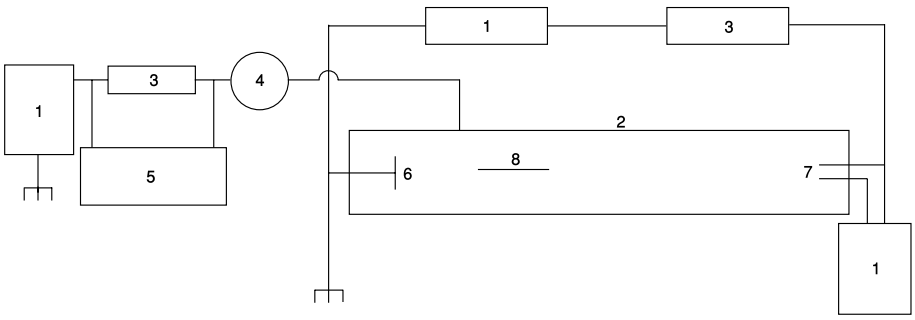

Fig. 1 The sketch of the experimental setup used to record the discharge current fluctuations in the tube filled with Helium, with (1) Power supply; (2) Glass tube; (3) Resistance; (4) Ampere meter; (5) A/D card and PC; (6) Anode plate; (7) Hot cathode; (8) Single Langmuir probe

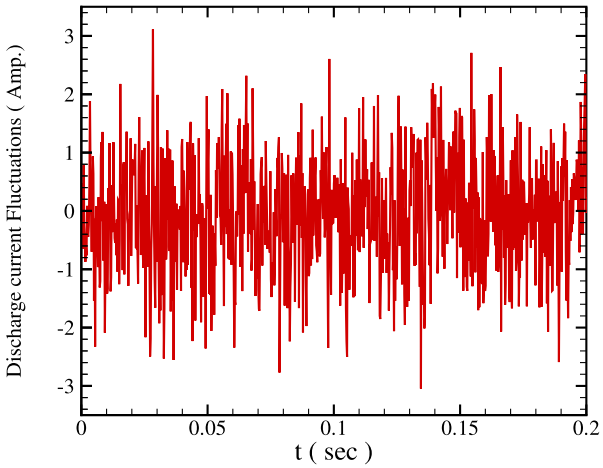

Fig. 2 Typical detrended electrical discharge current fluctuations in the plasma as a function of time

the other one represents the cathode (as a negative pole and electron propagator). The base pressure is 0.1 up to 0.8 Torr and the discharge tube is filled with Helium as the working gas under voltage of 400–900 V. The pressure, voltage and current should be fine tuned for ensuring the stability of the plasma. Using a resistor which was connected to an operational amplifier impedance converter, discharge current fluctuations are monitored. In this setup, we fixed the pressure and examined how the statistical properties of plasma change for various values of current. The fluctuations of the discharge current measured by single Langmuir probe were digitized and cleaned with a filter that omitted direct current. Finally, the fluctuation of the discharge were recorded by using an analog to digital card for several values of the electrical discharge current intensity, namely, 50, 60, 100, 120, 140, 180, and 210 mA at frequency equal to 44100 Hz. The resolution of recorded data is 12 bits. The typical size of the recorded data sets for each current intensity is about 10^6. Cleaned data were constructed by applying the Fourier-Detrended Fluctuation analysis. Figure 2 shows typical detrended discharge current fluctuation.

3 Markovian Nature of Data Set

As mentioned in the introduction, we use the Markovian method to explore the stochasticity nature of discharge current fluctuations in plasma. To investigate the Markovian nature of data, we briefly summarize the conceptions and theorems which will be importance for our statistical analysis of cleaned data set. For further details on Markov processes we refer the reader to the references [38, 39, 55–60].

We represent the discharge current fluctuations as a function of time by $X(t)$ and define $x(t) = X(t)/\sigma$, where σ is the standard deviation of discharge current fluctuations. Fundamental quantities related to the Markov processes are conditional probability density functions. The conditional probability density function (CPDF), $p(x_2, t_2|x_1, t_1)$, is defined as

$$p(x_2, t_2|x_1, t_1) = \frac{p(x_2, t_2; x_1, t_1)}{p(x_1, t_1)} \tag{1}$$

where $p(x_2, t_2; x_1, t_1)$ is the joint probability density function (JPDF), describing the probability of finding simultaneously, x_1 at scale(time), t_1, and x_2 at scale(time), t_2. Higher order

conditional probability densities can be defined in an analogous way

$$p(x_N, t_N|x_{N-1}, t_{N-1}; \ldots; x_1, t_1) = \frac{p(x_N, t_N; \ldots; x_1, t_1)}{p(x_{N-1}, t_{N-1}; \ldots; x_1, t_1)} \tag{2}$$

where $p(x_N, t_N; x_{N-1}, t_{N-1}; \ldots; x_1, t_1)$ is N-point joint probability density function. Intuitively, the physical interpretation of a Markov process is that it "forgets its past," or, in other words, only the most nearby conditioning, namely x_{N-1} at t_{N-1}, is relevant to the probability of finding a fluctuation x_N at t_N. Hence, in the Markov process the ability to predict the value of x_N will not be enhanced by knowing its values in the steps prior to the most recent one. So an important simplification that is made for a Markov process is that, the conditional multivariate joint PDF is written in terms of the products of simple two parameter conditional PDF's [55–57] as

$$p(x_N, t_N; x_{N-1}, t_{N-1}; \ldots; x_2, t_2|x_1, t_1) = \prod_{i=2}^{N} p(x_i, t_i|x_{i-1}, t_{i-1}) \tag{3}$$

To investigate whether underlying signal is a Markov process, one should tests the (3). But in practice for large values of N, is beyond the current computational capability. For $N = 3$ (three points or events), however, the condition will be

$$p(x_3, t_3|x_2, t_2; x_1, t_1) = p(x_3, t_3|x_2, t_2) \tag{4}$$

which should hold for any value of t_2 in the interval $t_1 < t_2 < t_3$. A process is then Markovian if the (4) is satisfied for a *certain* time separation $t_3 - t_2$, in which case, we define the Markov time scale as $t_{\text{Markov}} = t_3 - t_2$. For simplicity, we let $t_2 - t_1 = t_3 - t_2$. Thus, to compute the t_{Markov} we use a fundamental theory of probability according to which we write any three-point PDF in terms of the conditional probability functions as

$$p(x_3, t_3; x_2, t_2; x_1, t_1) = p(x_3, t_3|x_2, t_2; x_1, t_1)p(x_2, t_2; x_1, t_1) \tag{5}$$

Using the properties of Markov processes to substitute (5), we obtain

$$p_{\text{Mar}}(x_3, t_3; x_2, t_2; x_1, t_1) = p(x_3, t_3|x_2, t_2)p(x_2, t_2; x_1, t_1) \tag{6}$$

To determine the Markov time scale by means of joint probability density function ((5) and (6)), we use Bayesian statistics [61]. We introduce measurements and model parameters as $\{\mathcal{X}\} : \{p(x_3, t_3; x_2, t_2; x_1, t_1)\}$ and $\{\Theta\} : \{t_{\text{Markov}}\}$, respectively. Based on the Bayesian theorem, the conditional probability of the model parameters given data set (observation) is so-called posterior probability and is given by:

$$P(t_{\text{Markov}}|\mathcal{X}) = \frac{\mathcal{L}(\mathcal{X}|t_{\text{Markov}})P(t_{\text{Markov}})}{\int \mathcal{L}(\mathcal{X}|t_{\text{Markov}})P(t_{\text{Markov}})dt_{\text{Markov}}} \tag{7}$$

here $\mathcal{L}(\mathcal{X}|t_{\text{Markov}})$ is the so-called Likelihood and $P(t_{\text{Markov}})$ contains all initial constraints regarding to model parameters, so-called prior distribution expressed the degree of belief about the model. If we have no any extra information for model free parameters, the posterior function, $P(t_{\text{Markov}}|\mathcal{X})$ is proportional to the Likelihood function. Usually one can consider the various measurements to be independent of each other, so according to the central limit theorem, Likelihood function reads as:

$$\mathcal{L}(\mathcal{X}|t_{\text{Markov}}) \sim \exp\left(\frac{-\chi^2(t_{\text{Markov}})}{2}\right) \tag{8}$$

where:

$$\chi^2(t_{\text{Markov}}) = \int dx_1 dx_2 dx_3 [p(x_3, t_3; x_2, t_2; x_1, t_1) - p_{\text{Mar}}(x_3, t_3; x_2, t_2; x_1, t_1)]^2 / [\sigma^2_{3\text{-joint}} + \sigma^2_{\text{Mar}}] \quad (9)$$

$\sigma^2_{3\text{-joint}}$ and σ^2_{Mar} are the variances of $p(x_3, t_3; x_2, t_2; x_1, t_1)$ and $p_{\text{Mar}}(x_3, t_3; x_2, t_2; x_1, t_1)$, respectively. Evidently, when, for a set of values of the parameters, the $\chi^2(t_{\text{Markov}})$ is minimized, the probability will be maximized. The minimum value of $\chi^2_\nu(t_{\text{Markov}})$ ($\chi^2_\nu(t_{\text{Markov}}) = \chi^2(t_{\text{Markov}})/\mathcal{N}$, with $\mathcal{N}$ being the number of degree of freedom) corresponds to the best value of t_{Markov} for different value of electrical discharge current intensities.

The value of error-bar at 1σ confidence interval of t_{Markov} for each current intensity is determined by the Likelihood function according to:

$$68.3\% = \int_{-\sigma^-}^{+\sigma^+} \mathcal{L}(\mathcal{X}|t_{\text{Markov}}) dt_{\text{Markov}} \quad (10)$$

The values of Markov time scales, t_{Markov} in terms of discharge current intensity have been plotted in Fig. 3. It must be pointed out that, the unit of t_{Markov} reported in this figure has been changed to the units of microsecond (μs) by using the rate of digitalization in the experimental setup, 44100 sample/sec.

One can write (6) as an integral equation, which is well-known as the Chapman-Kolmogorov (CK) equation

$$p(x_3, t_3|x_1, t_1) = \int dx_2 \; p(x_3, t_3|x_2, t_2) \; p(x_2, t_2|x_1, x_1) \quad (11)$$

We have checked the validity of the CK equation for describing the time scale separation of t_1 and t_2 being equal to the Markov time scale. This is shown in Fig. 4 (for the data set with electrical current intensity, $I = 50$ mA). In this figure, the upper panel shows the contour plot of identification of the left (solid line) and right (dashed line) sides of (11) for two levels, 0.080 (inner contour) and 0.005 (outer contour). The conditional PDF $p(x_3, t_3|x_1, t_1)$, for $x_1 = \pm 1.25\sigma$, are shown in the lower panel. All the scales are measured in unit of the standard deviation of the discharge current fluctuations. We must point out that if all situations to be same as our experimental setup such as pressure, current intensity and so on, one can expect that all values derived by Markov analysis would be repeated. The value of

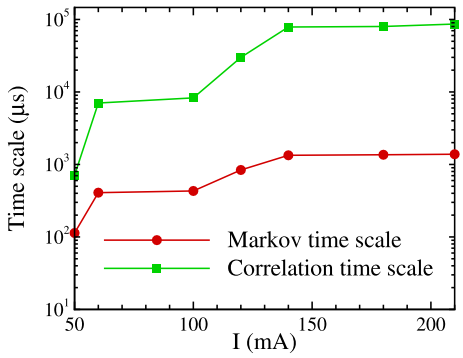

Fig. 3 Markov and correlation time scales as a function of discharge current intensity. The unit of vertical axis is microsecond

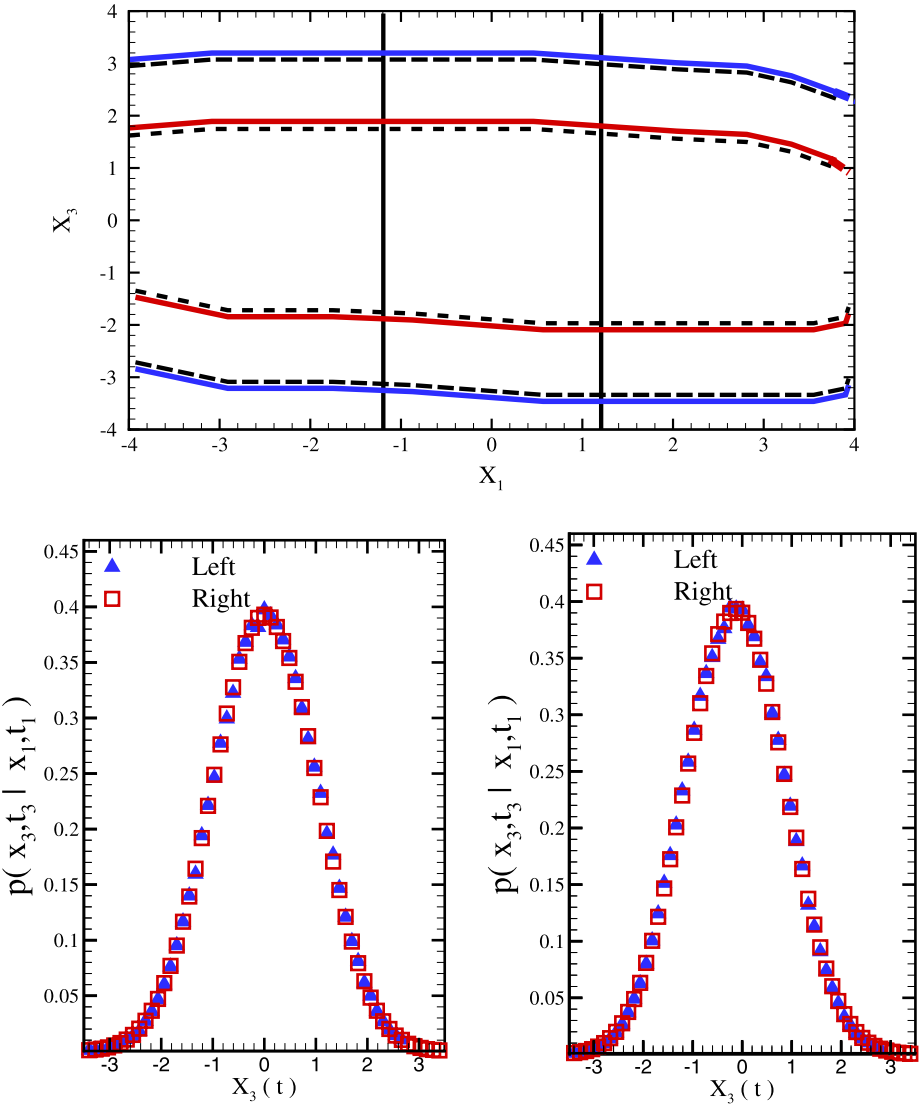

Fig. 4 *Upper panel* shows contour plots of the conditional PDF, $p(x_3, t_3|x_1, t_1)$. The *solid* and *dashed line* correspond to the left and right hand side of (11) for $t_3 - t_1 = 2 \times t_{\text{Markov}}$, respectively. Inner contours are a cutting of PDF at 0.08 level and outer contours correspond to 0.005 level. *Lower panel* corresponds to the cuts through the conditional PDF for $x_1 = \pm 1.25\sigma$

Markov time scale increases as discharge current intensity increases (see Fig. 3). It seems that by increasing the current intensity, charges become more energetic, therefore their effective cross-section will decrease and hence increasing their memory.

Up to now we determined the Markov time scale for each cleaned data set over which time series behaves as a Markov process. In the next section we will turn to the deriving master and stochastic equations governing the evolution of probability density function and fluctuation itself, respectively.

4 The Langevin Equation: Evolution Equation to Describe the Plasma Discharge Current Fluctuations

The Markovian nature of the plasma electrical discharge fluctuations enables us to derive a Fokker-Planck equation—a truncated Kramers-Moyal equation—for the evolution of the PDF $p(x,t)$, in terms of time t. The Chapman-Kolmogorov (CK) equation, formulated in differential form, yields the following Kramers-Moyal (KM) expansion [55–57]

$$\frac{\partial}{\partial t}p(x,t) = \sum_{n=1}^{\infty}\left(-\frac{\partial}{\partial x}\right)^n [D^{(n)}(x,t)\,p(x,t)] \tag{12}$$

where $D^{(n)}(x,t)$ are called as the Kramers-Moyal's coefficients. These coefficients can be estimated directly from the moments, $M^{(n)}$, and the conditional probability distributions as

$$D^{(n)}(x,t) = \frac{1}{n!}\lim_{\Delta t\to 0} M^{(n)} \tag{13}$$

$$M^{(n)} = \frac{1}{\Delta t}\int dx'(x'-x)^n\, p(x', t+\Delta t|x,t) \tag{14}$$

For a general stochastic process, all Kramers-Moyal's coefficients are different from zero. According to the Pawula's theorem, however, the Kramers-Moyal expansion stops after the second term, provided that the fourth order coefficient $D^{(4)}(x,t)$ vanishes. In that case, the Kramers-Moyal expansion reduces to a Fokker-Planck equation (also known as the backwards or second Kolmogorov equation) [55–57]

$$\frac{\partial}{\partial t}p(x,t) = \left\{-\frac{\partial}{\partial x}D^{(1)}(x,t) + \frac{\partial^2}{\partial x^2}D^{(2)}(x,t)\right\}p(x,t) \tag{15}$$

Also the evolution equation for conditional probability density function is given by the above equation except that $p(x,t)$ is replaced by $p(x,t|x_1,t_1)$. Here $D^{(1)}$ is known as the drift term and $D^{(2)}$ as diffusion term which represents the stochastic part. The Fokker-Planck equation describes the evolution of probability density function of a stochastic process generated by the Langevin equation (we use the Itô's definition) [55–57]

$$\frac{\partial}{\partial t}x(t) = D^{(1)}(x,t) + \sqrt{D^{(2)}(x,t)}\,f(t) \tag{16}$$

where $f(t)$ is a random force, i.e. δ-correlated white noise in t with zero mean and Gaussian distribution, $\langle f(t)f(t')\rangle = 2\delta(t-t')$. Using (13) and (14), for collected data sets, we calculate drift, $D^{(1)}$, and diffusion, $D^{(2)}$, coefficients, shown in Fig. 5. It turns out that the drift coefficient $D^{(1)}$ is a linear function in x, whereas the diffusion coefficient $D^{(2)}$ is a quadratic function. For large values of x, our estimations become poor, the uncertainty increases, so we truncate our estimations up to 3σ of fluctuations as indicated in Fig. 5.

The functional feature of drift and diffusion coefficients for different electrical discharge data sets are reported in Table 1. To ensure that Kramers-Moyal expansion (12) reduces to a Fokker-Planck equation (15), we compute fourth-order coefficient $D^{(4)}$. In our analysis, $D^{(4)} \simeq 10^{-1}D^{(2)}$. One must point out that, however the fourth-order Kramers-Moyal's coefficient is not so small, but in the current analysis, this doesn't make measurable uncertainty in our results (see below). Furthermore, using (16), it becomes clear that we are able to

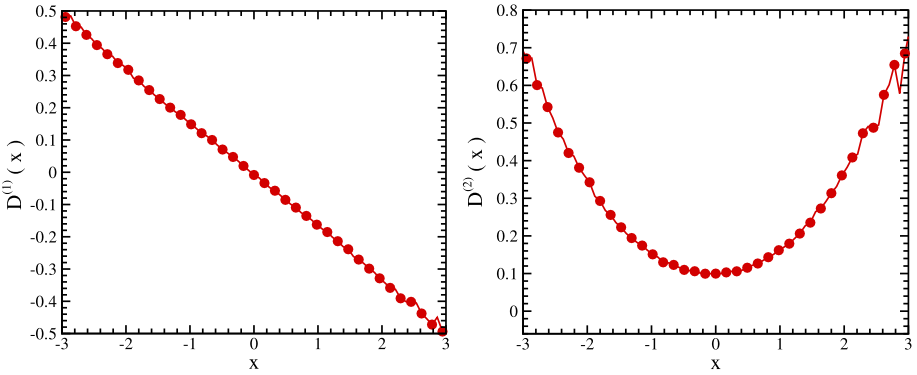

Fig. 5 Drift, $D^{(1)}(x)$, diffusion and $D^{(2)}(x)$ coefficients for data set with $I = 50$ mA

Table 1 The values of Kramers-Moyal coefficients for data set at different discharge current intensities

	$D^{(1)}(x)$	$D^{(2)}(x)$
50 mA	$-0.160\,x$	$0.090 + 0.003\,x + 0.070\,x^2$
60 mA	$-0.058\,x$	$0.026 + 0.002\,x + 0.030\,x^2$
100 mA	$-0.052\,x$	$0.026 + 0.002\,x + 0.026\,x^2$
120 mA	$-0.028\,x$	$0.013 + 0.001\,x + 0.014\,x^2$
140 mA	$-0.017\,x$	$0.008 + 0.001\,x + 0.009\,x^2$
180 mA	$-0.017\,x$	$0.008 + 0.001\,x + 0.009\,x^2$
210 mA	$-0.016\,x$	$0.009 + 0.001\,x + 0.008\,x^2$

separate the deterministic and the noisy components of the fluctuations in terms of the coefficients $D^{(1)}$ and $D^{(2)}$. According to the values of the Kramers-Moyal's coefficients reported in Table 1, it is possible to reconstruct discharge current fluctuations at arbitrary current intensity using (15) and (16) [7–10].

Now let us have a comparison of the statistical properties of reconstructed data using (16) with the original fluctuations. For this purpose, we rely on the solution of Fokker-Planck equation for conditional probability function (same as (15) for infinitesimally small step τ) which is given by [55–57]

$$p(x_2, t+\tau|x_1, t) = \frac{1}{2\sqrt{\pi\, D^{(2)}(x_1,t)\tau}} \exp\left(-\frac{(x_2 - x_1 - D^{(1)}(x_1,t)\tau)^2}{4D^{(2)}(x_1,t)\tau}\right) \tag{17}$$

Left panel of Fig. 6 shows conditional probability density function computed by the above equation and directly calculated from the original detrended data set for $I = 50$ mA. The plot from left to right correspond to $x_1 = -0.5\sigma$, $x_1 = 0.0$ and $x_1 = +0.5\sigma$ level, respectively. We also compute the conditional probability using reconstructed fluctuations via (16) and compare it with the same one for original cleaned data at three mentioned levels for x_1. We took $\tau = t_{\text{Markov}}$ for all plots in Fig. 6. According to (17) and based on Fig. 6 we find a good agreement between stochastic model for reconstructed plasma fluctuations and original fluctuations.

According to the definition of Markov time scale, there is no systematic relation between Markov and autocorrelation time scales, however one can decompose the temporal

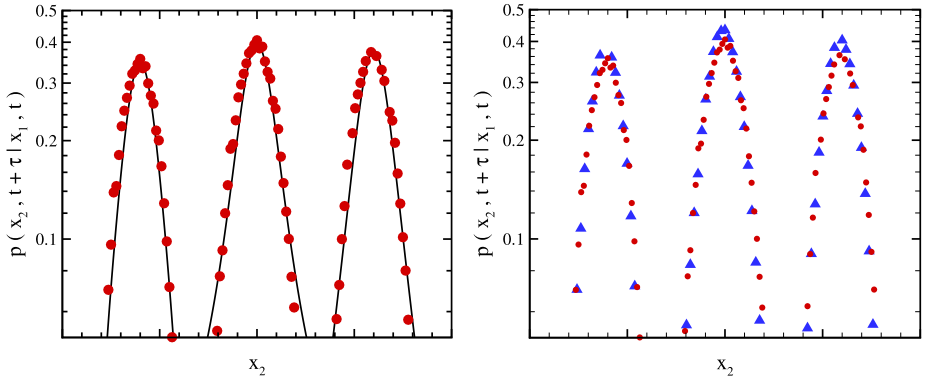

Fig. 6 *Left panel* corresponds to the conditional probability density function determined by analytical formula, (17) (*solid line*) and directly computed by original cleaned data (*symbol*) for $I = 50$ mA. *Right panel* shows the comparison between the conditional probability density function determined by generated data using (16) (*triangle symbol*) and our initial cleaned data (*circle symbol*). In each *panel*, the plots from *left* to *right* correspond to the cut for $x_1 = -0.5\sigma$, $x_1 = 0.0$ and $x_1 = +0.5\sigma$ level, respectively. To make more obvious, we shifted the value of x_2 for each plot. We took $\tau = t_{\text{Markov}}$, where t_{Markov} is the Markov time scale of data set

correlation function of an arbitrary stationary Markov processes according to the formalism introduced by Medvedev [62]. To this end, we introduce temporal correlation function as:

$$\mathcal{C}(x_1(t_1), x_2(t_2)) = \langle x_1(t_1)x_2(t_2)\rangle \tag{18}$$

here the sign $\langle . \rangle$, shows the ensemble averaging. We have set the mean of time series equal to zero. For a stationary time series the correlation function depends on only the separation time scale, which means that

$$\mathcal{C}(\tau) \equiv \mathcal{C}(x_1(t_1), x_2(t_2)) = \langle x_1(t_1)x_2(t_1+\tau)\rangle \tag{19}$$

In the presence of any trends and nonstationarity, correlation function depends not only to the time separation $(t_2 - t_1)$, but also to the starting and finishing times, namely t_1 and t_2, respectively. As demonstrated in [6], the underlying detrended data for discharge current behaves as a stationary signal. The temporal correlation function for plasma detrended data with $I = 50$ mA is plotted in the left hand side of the Fig. 7. This figure confirms the underlying data sets behave as an anti-correlated series which has been confirmed in [6] using another method. We also present the same plot for a pure random white noise data, i.e. with Hurst exponent $H = 0.5$, in the right hand side of the Fig. 7 for comparison. As explained before the evolution of a typical stationary Markov process is governed by Master equation (12), so the temporal correlation function of this process can be written as:

$$\langle x(t+\tau)x(t)\rangle = \sum_{m=0}^{\infty} \frac{|\tau|^m}{m!}\langle x\mathcal{F}^m x\rangle \tag{20}$$

here $\mathcal{F} = \sum_{n=1}^{\infty} \frac{D^{(n)}(x,t)}{n!}\frac{\partial^n}{\partial x^n}$. To calculate temporal correlation function of a Markov process, we should compute probability density of data set. The solution of (15) is:

$$p(x,t) = \frac{\text{const.}}{\sqrt{D^{(2)}(x,t)}} \exp\left(-\int \frac{D^{(1)}(x,t)}{D^{(2)}(x,t)}dx\right) \tag{21}$$

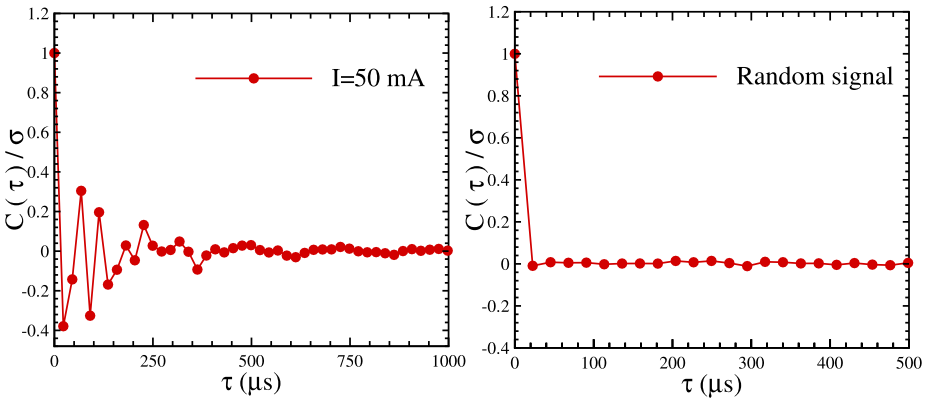

Fig. 7 Normalized temporal correlation function for plasma cleaned data for discharge current with $I = 50$ mA (*left panel*) and for completely random data (*right panel*)

If one use the following parameterizations for

$$D^{(1)}(x,t) = ax(t) \quad \text{and} \quad D^{(2)}(x,t) = b + cx(t) + dx^2(t),$$

then can find:

$$p(x,t) = \frac{\text{const.}}{\sqrt{D^{(2)}(x,t)}} \exp\left(\frac{a \ln[b + cx(t) + dx^2(t)]}{2d} - \frac{ac \arctan\left(\frac{c+2dx(t)}{\sqrt{4bd-c^2}}\right)}{d\sqrt{4bd-c^2}} \right) \tag{22}$$

The constant coefficient could be determined by normalization procedure. Obviously for $c, d = 0$ above probability density function behaves as a Gaussian distribution. According to the Kramers-Moyal coefficients reported in Table 1 for the plasma fluctuations, we expect the probability density functions for various discharge current intensity deviate from exact Gaussian function. As an example, one can simply show that the temporal correlation function of a stochastic variable, $x(t)$, governed by the Langevin equation

$$\dot{x}(t) = -\gamma x(t) + \eta(t)$$

behaves as:

$$\langle x(t+\tau)x(t)\rangle \sim e^{-\gamma\tau} \tag{23}$$

consequently one can introduce temporal correlation scale as γ^{-1} while for this process, Markov length scale equates to unity [62]. This shows that for our data set the correlation time scale is greater or equal to the Markov time scale. In Fig. 3, we estimate the temporal correlation scale at stationary case of plasma fluctuations by using $D^1(x,t)$ reported in Table 1. In addition for a scaling behavior of autocorrelation function, namely $\langle x(t+\tau)x(t)\rangle \sim \tau^{-\kappa}$, in terms of Hurst exponent, one can find out the scaling exponent for autocorrelation function as $\kappa = 2 - 2H$. Then by increasing Hurst exponent, κ decreased and degree of correlation to be increased (see e.g. [6]). Our results show that Markov time scale is almost an increasing function versus discharge current intensity which directly reflects the memory in the stochastic current fluctuations produced in plasma measured by Langmuir probe.

5 Non-Gaussianity and Multifractality of Plasma Fluctuations

In this section we investigate the Gaussian nature of the PDFs of reconstructed and detrended time series as well as its multifractal exponent derived by Markovian approach. For a Gaussian distribution, all the even moments are related to the second moment through $\langle x^{2n}\rangle = \frac{2n!}{2^n n!}\langle x^2\rangle^n$ (e.g., for $n=2$, $\langle x^4\rangle = 3\langle x^2\rangle^2$), while the odd moments are zero identically. We can directly check the relation between the higher moments for the plasma fluctuations data at different value of discharge current intensities with second moment. The values of moments and their variances calculating directly from data are summarized in Table 2.

Let us examine the predictions for the moments of the plasma fluctuations via the Fokker-Planck equation, and compare their values with the direct evaluation represented in the Table 2. Using the general Kramers-Moyal expansion, (12), which is also valid for the probability density $p(x,t)$, differential equations for the n-th order moments can be derived. By multiplication of the both side of (12) with x^n and integration with respect to x, we can obtain evolution of different moments of data set as:

$$\begin{aligned}\frac{d}{dt}\langle x^n(t)\rangle &= \sum_{k=1}^{\infty}(-1)^k\int_{-\infty}^{+\infty} x^n\left(\frac{\partial}{\partial x}\right)^k D^{(k)}(x,t)p(x,t)dx\\ &= \sum_{k=1}^{n}\frac{n!}{(n-k)!}\int_{-\infty}^{+\infty} x^{n-k}D^{(k)}(x,t)p(x,t)dx\\ &= \sum_{k=1}^{n}\frac{n!}{(n-k!)}\left\langle x^{n-k}D^{(k)}(x,t)\right\rangle \end{aligned} \tag{24}$$

We put $n=4$ in the above equation and find the equation for the fourth moment as follows

$$\begin{aligned}\frac{d}{dt}\langle x^4(t)\rangle &= 4\langle D^{(1)}(x)x^3(t)\rangle + 12\langle D^{(2)}(x)x^2(t)\rangle\\ &\quad + 24\langle D^{(3)}(x)x(t)\rangle + 24\langle D^{(4)}(x)\rangle\end{aligned} \tag{25}$$

Table 2 The values of moments, $\langle x^n\rangle$, and their errors for data set at different discharge current intensities

	$\langle x^2\rangle \times 10^{+5}$	$\langle x^3\rangle \times 10^{+9}$	$\langle x^4\rangle \times 10^{+9}$
50 mA	2.483 ± 0.001	-0.395 ± 0.417	1.842 ± 0.062
60 mA	2.415 ± 0.001	-3.330 ± 0.123	1.532 ± 0.001
100 mA	2.879 ± 0.001	-17.500 ± 1.990	4.140 ± 0.318
120 mA	2.600 ± 0.001	-3.140 ± 0.179	1.858 ± 0.008
140 mA	2.095 ± 0.001	-5.770 ± 0.380	1.431 ± 0.030
180 mA	1.617 ± 0.001	-7.220 ± 2.850	2.002 ± 0.765
210 mA	1.383 ± 0.001	-0.458 ± 0.139	0.811 ± 0.335

Table 3 The values of third and fourth Kramers-Moyal coefficients for data set at different discharge current intensities

	$D^{(3)}(x)$	$D^{(4)}(x)$
50 mA	$-0.007 - 0.073\,x$ $-0.019\,x^3$	$0.009 + 0.009\,x + 0.010\,x^2$ $-0.001\,x^3 + 0.001\,x^4$
60 mA	$-0.024\,x - 0.002\,x^2$ $-0.010\,x^3$	$0.001 - 0.020\,x + 0.010\,x^2$ $+0.001\,x^3 + 0.003\,x^4$
100 mA	$-0.025\,x - 0.001\,x^2$ $-0.009\,x^3$	$0.002 + 0.001\,x + 0.013\,x^2$ $+0.002\,x^4$
120 mA	$-0.013\,x - 0.005\,x^3$	$0.001 + 0.006\,x^2 + 0.001\,x^4$
140 mA	$-0.008\,x - 0.003\,x^3$	$0.0009 + 0.003\,x^2 + 0.001\,x^4$
180 mA	$-0.007\,x - 0.003\,x^3$	$0.0007 + 0.002\,x^2 + 0.001\,x^4$
210 mA	$-0.009\,x - 0.002\,x^3$	$0.0008 + 0.005\,x^2$

Table 4 The values of α's coefficients and their variances, σ's, for data set at different discharge current intensities

	α_2	σ_2	α_3	σ_3
50 mA	3.14	0.38	0.18	0.21
60 mA	3.81	0.70	−1.17	0.51
100 mA	2.86	0.53	−3.68	0.66
120 mA	2.77	0.98	2.25	0.96
140 mA	3.05	0.56	−2.09	0.35
180 mA	3.67	0.85	−0.01	0.28
210 mA	3.08	0.95	−4.18	0.95

The third and fourth Kramers-Moyal's coefficients for the data set are reported in Table 3. We should point out that the values of $|D^{(3)}|$ and $|D^{(4)}|$ are less than $|D^{(2)}|$. For the stationary case, all the moments of fluctuations are time independent and the left-hand side of (25) vanishes, so

$$\langle x^4\rangle = [\alpha_2(I) \pm \sigma_2(I)]\langle x^2\rangle^2 + [\alpha_3(I) \pm \sigma_3(I)]\langle x^3\rangle\sqrt{\langle x^2\rangle} \tag{26}$$

where $\alpha_2(I)$ determines the coefficient of kurtosis quantity and $\sigma_2(I)$ shows its variance. Also $\alpha_3(I)$ determines the coefficient of skewness and $\sigma_3(I)$ indicates its error. The skewness measures the asymmetry of probability density function and kurtosis determines the statistic of rare events in the processes. In generally they may depend to the discharge current intensity, I. Using the results represented in the Table 3, for each case of fluctuations $\alpha_n(I)$ and its variance are given in the Table 4.

As we mentioned before, for exact Gaussian process, we should have

$$\alpha_2(I) = \frac{\langle x^4\rangle}{\langle x^2\rangle^2} = 3.0 \tag{27}$$

$$\alpha_3(I) = 0.0 \tag{28}$$

If $\alpha_2(I) > 3.0$ means that probability density function has fat tail and rare events have more chance to occur (with respect to the Gaussian process). While for $\alpha_2(I) < 3.0$, the tails of probability density function is heavy than the Gaussian distribution. According to the values of $\alpha_2(I)$ and $\alpha_3(I)$, we find that probability density function of data set is deviated

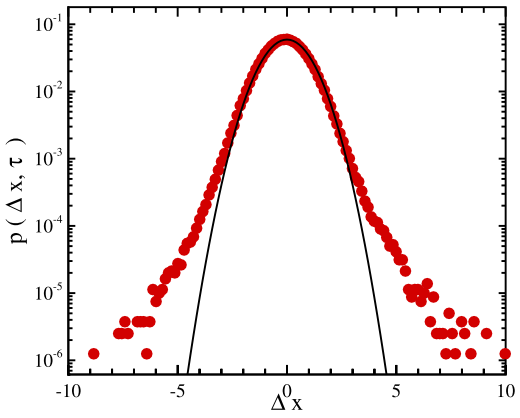

Fig. 8 Probability density function of reconstructed increment data set (*filled symbols*) and a typical Gaussian function (*solid line*) for $I = 50$ mA and $\tau = 1$

from Gaussian. This deviation can be characterized by skewness as well as kurtosis coefficients [63]. Table 4 demonstrates that there is no monotonous behavior for deviations from Gaussianity as a function of discharge current intensity [64, 65]. Subsequently the properties of probability density function appears almost independent of the plasma conditions [66]. In this case, we expect that the increment of signals also may reveal the non-Gaussianity properties. To this end, we introduce increment series as $\Delta x(\tau) \equiv x(t+\tau) - x(t)$, where τ is time delay. We do the same computation to determine whether this new data set has Markovian nature. Our analysis demonstrate that Markov time scale of $\Delta x(\tau)$ for all discharge current intensity is 136^{+90}_{-45} μs. Figure 8 shows the probability density of reconstructed increment data set with a typical time lag equates to $\tau = 1$ for $I = 50$ mA. If the probability density function to be fatter than Gaussian function hence the probability of observing fluctuations far exceeding the average amplitude are not ignorable. This phenomenon can affect on usual transport in the plasma.

To check the multifractal nature of reconstructed time series, we investigate the Markovian nature of the increments of profile which is defined as: $\Delta x(\tau) \equiv y(t+\tau) - y(t)$, where $y(t) = \sum_{i=0}^{t} x(i)$. For convenience, hereafter we rename $y(t)$ by $x(t)$. According to the mentioned procedure, we can determine the Markov time scales for the increments and calculate the Kramers-Moyal's coefficients. Likelihood analysis confirms that, the increment of profile signal for all electrical current intensities are also Markov processes.

The Fokker-Planck equation for probability density function of the increment is given by [38, 67]

$$-\tau \frac{\partial}{\partial \tau} p(\Delta x, \tau) = \left\{ -\frac{\partial}{\partial \Delta x} D^{(1)}(\Delta x, \tau) + \frac{\partial^2}{\partial \Delta x^2} D^{(2)}(\Delta x, \tau) \right\} p(\Delta x, \tau) \tag{29}$$

the negative sign of the left-hand side of (29) is due to the direction of the cascade from large to smaller time scales τ. The corresponding Langevin equation can be read as

$$-\tau \frac{\partial}{\partial \tau} \Delta x(\tau) = D^{(1)}(\Delta x, \tau) + \sqrt{D^{(2)}(\Delta x, \tau)}\, f(\tau) \tag{30}$$

where $f(\tau)$ is the same as random function in (16). For time series with scaling correlations the drift and diffusion coefficients of increment are formulated as [38, 67, 68]

$$\begin{aligned} D^{(1)}(\Delta x, \tau) &\simeq -H \Delta x \\ D^{(2)}(\Delta x, \tau) &\simeq b \Delta x^2 \end{aligned} \tag{31}$$

Using (29) and (31) we obtain the evolution of structure functions as: $(S_q(\tau) \equiv \langle|\Delta x(\tau)|^q\rangle = \langle|x(t+\tau)-x(t)|^q\rangle)$ as follows

$$-\tau\frac{\partial}{\partial\tau}\langle|\Delta x(\tau)|^q\rangle = q\langle|\Delta x(\tau)|^{q-1}D^{(1)}(\Delta x,\tau)\rangle + q(q-1)\langle|\Delta x(\tau)|^{q-2}D^{(2)}(\Delta x,\tau)\rangle \tag{32}$$

by substituting the (31) in (32) we find

$$\tau\frac{\partial}{\partial\tau}\langle|\Delta x(\tau)|^q\rangle = [qH - bq(q-1)]\langle|\Delta x(\tau)|^q\rangle \tag{33}$$

the above equation implies scaling behavior for moments of increments, structure function as

$$S_q(\tau) \equiv \langle|\Delta x(\tau)|^q\rangle = \langle|x(t+\tau)-x(t)|^q\rangle \sim \tau^{\xi(q)}. \tag{34}$$

According to (33) and (34), the corresponding scaling exponent in general case can be read as

$$\xi(q) = qH - bq(q-1) \tag{35}$$

For mono- and multi-fractal processes the exponent $\xi(q)$ have linear and non-linear behavior with q, respectively. It must point out that H is nothing except the underlying fluctuations's Hurst exponent [69–72]. The obtained expression for $D^{(1)}(\Delta x,\tau)$ and $D^{(2)}(\Delta x,\tau)$ (to avoid the overissue we just report the results of data for $I = 50$ mA) are as follows

$$\begin{aligned} D^{(1)}(\Delta x,\tau) &= -(0.45\pm0.03)\Delta x \\ D^{(2)}(\Delta x,\tau) &= (0.04\pm0.01)\Delta x^2 \end{aligned} \tag{36}$$

consequently, using (36) and (35), the scaling exponent is determined as

$$\xi(q) = (0.45\pm0.03)q - (0.04\pm0.01)q(q-1) \tag{37}$$

To check the consistency of estimated scaling exponent $\xi(q)$, (37), with that of determined by original time series we use the extended self similarity (ESS) method [73, 74]. Extended Self Similarity is a method to find an extended range of scaling behavior of underlying stochastic fluctuations. The prediction of Kolmogorov (K41) theory for the velocity field of fully developed turbulence namely in the inertial regime is $S_q(\tau) \sim \tau^{\xi_q}$ with $\xi_q = \frac{q}{3}$ and shows a nonofractal behavior [75]. The deviation from this prediction have been reported experimentally and theoretically, due to the energy dissipation fluctuations (see [74, 76–80]). In the context of Extended Self Similarity, the self similarity expressed above to be changed to a new scaling relation according to $S_q \sim S_3^{\zeta_q}$ in which not only the scaling regime for self similarity behavior to be extended even further from inertia range, but also the statistical uncertainty for determining scaling exponent decreases. In the Extended Self Similarity method, the log-log plot of $S_q(\tau)$ as a function of specific order of structure function, namely $S_3(\tau)$, usually shows an extended scaling regime

$$S_q(\tau) \sim S_3(\tau)^{\zeta(q)} \tag{38}$$

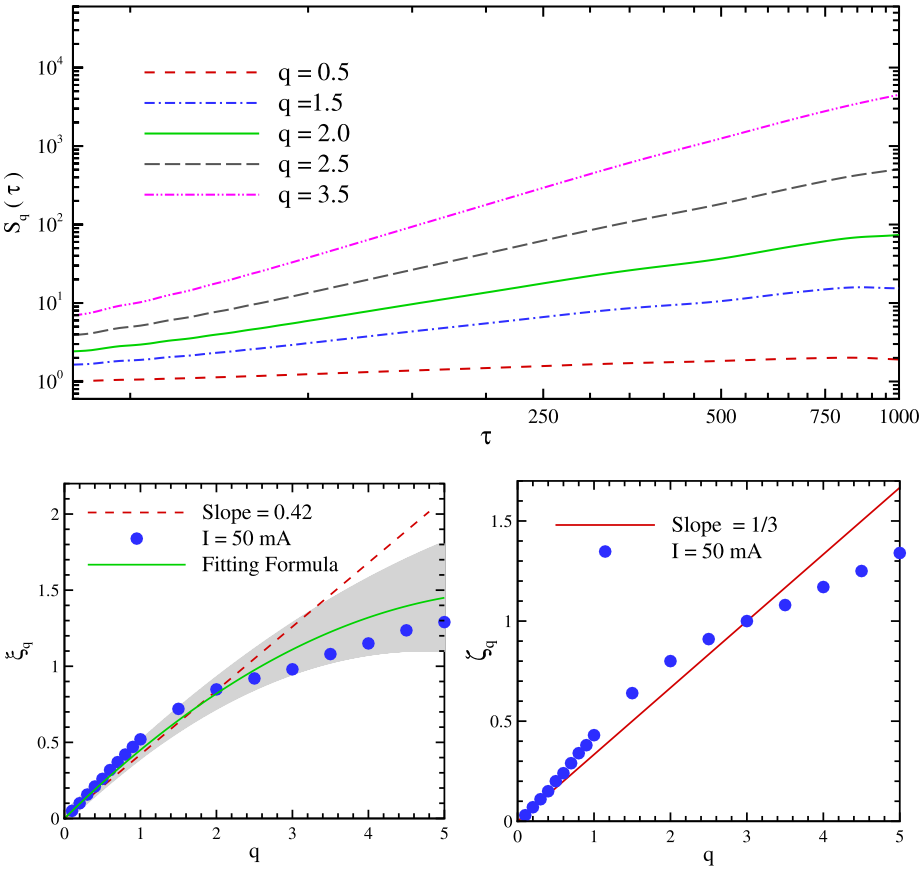

Fig. 9 *Upper panel* indicates the structure function versus τ. *Lower left panel* shows the scaling exponent of $S_q(\tau)$ as a function of moment for original cleaned plasma fluctuations (*filled symbol*) and *solid line* corresponds to the fitting formula derived by Kramers-Moyal's coefficients for multi-fractal anti-correlated signal with $H = 0.42$ (see (37)). Also in this *panel*, *dashed line* corresponds to a mono-fractal anti-correlated series. *Lower right panel* indicates $\zeta(q)$ versus q. Here we chose the data set with $I = 50$ mA

For any Gaussian process, the exponent in the above equation is given by $\zeta(q) = q/3$ [73, 74]. Any deviation from this relation can be interpreted as a deviation from Gaussianity. Figure 9 shows the log-log plot of structure function in terms of time scaling (upper panel), exponents $\xi(q)$ (left lower panel) and $\zeta(q)$ (right lower panel) for the plasma fluctuations with $I = 50$ mA. The present results are in agrement with our previous results derived that the plasma time series have multi-fractal nature [6].

As shown in the lower left panel of Fig. 9, (37) for $\xi(q)$ (solid line) with the shaded area corresponds to 68.3% confidence interval derived by Markovian analysis of increment of profile has an acceptable confidence level to experimental results (filled symbol).

6 Summary and Conclusion

Many methods have been devoted to study the fluctuations in the plasma [81–85]. Since, discharge current fluctuations can serve as a quantitative indicator of plasma disturbances,

consequently any tantalizing statistical evidences give new insight throughout plasma fluctuations. We have studied the stochastic nature of the electrical discharge current fluctuations in the Helium plasma as a working gas. As mentioned before, fluctuations measured by Langmuir probe assimilate stochastic phenomena occurred in a typical plasma fluid. Therefore it can reveal many interesting feature which can not investigated by common methods in data analyzing. We have applied the Fourier-Detrended Fluctuations Analysis method to extract sinusoidal trend and used clean data set for further analysis [6].

Here we used the novel approach i.e. the Markovian method to investigate many statistical properties of the current fluctuations in the plasma. We showed that how the mathematical framework of Markov processes can be applied to develop a successful statistical description of the plasma fluctuations. We have analyzed detrended data via Markovian method. The Markov time scale, as the characteristic time scale of the Markov properties of the electrical discharge current fluctuations, was obtained. According to the theory of the stochastic process, the electrical discharge fluctuations at time scales larger than the Markov time scale can be considered as a Markov process. This means that the data located at the separations larger than the Markov time scale can be described as a Markov chain. It is found that Markov time scale, t_{Markov} increases by increasing the current intensity in the plasma. This means that the memory of charged particles in the plasma increase as current intensity increases. It is due to the fact that particles become more energetic, therefore they can penetrate deeper in the plasma without considerable deviation from the initial trajectory. In other words, by increasing discharge current density the electron impact ionization cross section almost decreases, consequently it is statistically expected that memory of electrons at this mesoscale for energy transfer to be decreased causing the drift as well as diffusion coefficients of current fluctuations to be reduced [86–88].

Using the Markovian nature of fluctuations, we demonstrated that, the probability density function of fluctuations satisfies a Fokker-Planck equation. Based on this equation one can do averaging to extract relevant observable quantities of plasma fluctuations. The so-called Kramers-Moyal's coefficients by using conditional moments (14) have been determined. The Langevin equation, governing the evolution of current fluctuations has also been given. To check the consistency of statistical properties of regenerated data set with original cleaned series, we compare conditional probability density function derived by (17) with that of computed by original data in Fig. 6.

By using exact decomposition of temporal correlation function for stationary Markov processes, we gave an expression (20) to determine correlation function of plasma fluctuations. For the stationary time series, we calculated correlation time scale which in principle differs from Markov characteristic time scale. We argued that there is no systematic relation between Markov and correlation time scales. It must point out that, Markov time scale is potentially related to energy transfer in mesoscale dynamics. Also here based on Markovian method we gave an equation for evolution of various moments of structure function (24). As we expected from (22), a deviation from Gaussianity has been observed. This might give a hint toward the multifractality nature of plasma fluctuations in our set up. Our results confirm that plasma fluctuations in all range of current intensity prepared in our set up behave as non-Gaussian processes. To extend the scaling behavior of $S_q(\tau)$ versus τ, we relied on Extended Self Similarity method. Extended Self Similarity approach confirmed that, the scaling exponents of the discharge current fluctuations didn't follow the Kolmogorov (K41) scaling exponents. It means that there is no constant energy cascade form large scales (time or space) to small one and there exists energy dissipation fluctuations in the plasma.

Acknowledgements Authors would like to thank S. Sobhanian for useful comments and discussions.

References

1. Ghasemi, F., Bahraminasab, A., Sadegh Movahed, M., Rahvar, S., Sreenivasan, K.R., Rahimi Tabar, M.: J. Stat. Mech. P11008 (2006)
2. Garscadden, A., Emeleus, K.G.: Proc. Phys. Soc. **79**, 535 (1962)
3. Ding, W.X., Klinger, T., Piel, A.: Phys. Lett. A **222**(6), 409 (1996)
4. Gyergyek, T.: Plasma Phys. Control. Fusion **41**, 175 (1999)
5. Letellier, C., Menard, O., Klinger, T., Piel, A., Bonohomme, G.: Physica D **156**, 169 (2001)
6. Kimiagar, S., Sadegh Movahed, M., Khorram, S., Sobhanian, S., Reza Rahimi Tabar, M.: J. Stat. Mech. P03020 (2009)
7. Friedrich, R., Peinke, J.: Phys. Rev. Lett. **78**, 863 (1997)
8. Davoudi, J., Reza Rahimi Tabar, M.: Phys. Rev. Lett. **82**, 1680 (1999)
9. Jafari, G.R., Fazeli, S.M., Ghasemi, F., Vaez Allaei, S.M., Tabar, M.R., Iraji Zad, A., Kavei, G.: Phys. Rev. Lett. **91**, 226101 (2003)
10. Sangpour, P., Akhavan, O., Moshfegh, A.Z., Jafari, G.R., Reza Rahimi Tabar, M.: Phys. Rev. B **71**, 155423 (2005)
11. Waechter, M., Riess, F., Kantz, H., Peinke, J.: Europhys. Lett. **64**(5), 579 (2003)
12. Friedrich, R., Peinke, J., Reza Rahimi Tabar, M.: In Meyers, B. (ed.) Contribution to Encyclopedia of Complexity and System Science, p. 3574. Springer, Berlin (2009),
13. Friedrich, R., Peinke, J., Sahimi, M., Reza Rahimi Tabar, M.: Phys. Rep., in press
14. Shayeganfar, F., Jabbari-Farouji, S., Movahed, M.S., Jafari, G.R., Reza Rahimi Tabar, M.: Phys. Rev. E **81**, 061404 (2010)
15. Farahzadi, A., Niyamakom, P., Beigmohammadi, M., Mayer, N., Heuken, M., Ghasemi, F., Reza Rahimi Tabar, M., Michely, T., Wuttig, M.: Europhys. Lett. **90**, 10008 (2010)
16. Shayeganfar, F., Jabbari-Farouji, S., Sadegh Movahed, M., Jafari, G.R., Reza Rahimi Tabar, M.: Phys. Rev. E **80**, 061126 (2009)
17. Manshour, P., Saberi, S., Sahimi, M., Peinke, J., Pacheco, A.F., Reza Rahimi Tabar, M.: Phys. Rev. Lett. **102**, 014101 (2009)
18. Ghasemi, F., Sahimi, M., Peinke, J., Friedrich, R., Reza Jafari, G., Reza Rahimi Tabar, M.: Phys. Rev. E **75**, R060102 (2007)
19. Farahpour, F., Eskandari, Z., Bahraminasab, A., Jafari, G.R., Ghasemi, F., Sahimi, M., Reza Rahimi Tabar, M.: Physica A **385**, 601–608 (2007)
20. Jafari, G.R., Sadegh Movaged, M., Noroozzadeh, P., Bahraminasab, A., Sahimi, M., Ghasemi, F., Reza Rahimi Tabar, M.: Int. J. Mod. Phys. C **18**, 1689 (2007)
21. Jafari, G.R., Reza Rahimi Tabar, M., Iraji zad, A., Kavei, G.: J. Phys. A **375**, 239 (2007)
22. Ghasemi Muhammad Sahimi, M., Peinke, J., Reza Rahimi Tabar, M.: J. Biol. Phys. **32**, 117–128 (2006)
23. Shahbazi, F., Sobhanian, S., Reza Rahimi Tabar, M., Khorram, S., Frootan, G.R., Zahed, H.: J. Phys. A, Math. Gen. **36**(10), 2517–2524 (2003)
24. Ghasemi, F., Peinke, J., Sahimi, M., Rahimi Tabar, M.R.: Eur. Phys. J. B **47**, 411 (2005)
25. Chianca, C.V., Ticona, A., Penna, T.J.P.: Physica A **357**(3–4), 447 (2005)
26. Kantelhardt, J.W., Koscielny-Bunde, E., Rego, H.H.A., Havlin, S., Bunde, A.: Physica A **295**, 441 (2001)
27. Li, B., Hazeltine, R.D., Gentle, K.W.: Phys. Rev. E **76**, 066402 (2007)
28. Li, B., Hazeltine, R.D.: Phys. Rev. E **73**, 065402R (2006)
29. Sigeneger, F., Winkler, K.: Appl. Phys. **19**(3), 211–223 (2002)
30. Isupov, A.V., Ulanov, I.M.: High Temp. **43**(2), 169 (2005)
31. Denysenko, I., et al.: Phys. Plasmas **13**, 073507 (2006)
32. Carreras, B.A., et al.: Phys. Plasmas **7**, 3278 (2000)
33. Budaev, V.P., Dufkova, E., Nanobashvili, S., Weinzettl, V., Zajac, J.: In: 32nd EPS Conference on Plasma Phys. Tarragona, ECA 29C, P-5.019, 27 June–1 July (2005)
34. Budaev, V.P.: Phys. A: Stat. Mech. Appl. **344**, 299–307 (2004)
35. Pedrosa, M.A., et al.: Phys. Rev. L **82**, 18 (1999)
36. Siegert, S., Friedrich, R., Peinke, J.: Phys. Lett. A **243**(5–6), 275–280 (1998)
37. Friedrich, R., Peinke, J.: Phys. Rev. Lett. **78**(5), 863 (1997)
38. Friedrich, R., Peinke, J., Renner, C.: Phys. Rev. Lett. **84**(22), 5224 (2000)
39. Friedrich, R., Marzinzik, K., Schmigel, A.: In: Parisi, J., Muller, C.S., Zimmermann, W. (eds.) A Perspective Look at Nonlinear Media. Lecture Notes in Physics, vol. 503, p. 313. Springer, Berlin (1997)
40. Friedrich, R., Renner, C., Siefert, M., Peinke, J.: Phys. Rev. Lett. **89**, 149401 (2002)
41. Ma, Q.D.Y., Bartsch, R.P., Bernaola-Galvan, P., et al.: Phys. Rev. E **81**, 031101 (2010)
42. Xu, L.M., Ivanov, P.C., Hu, K., et al.: Phys. Rev. E **71**, 051101 (2005)
43. Hu, K., Ivanov, P.C., Chen, Z., Carpena, P., Stanley, H.E.: Phys. Rev. E **64**, 011114 (2001)
44. Chen, Z., Ivanov, P.C., Hu, K., et al.: Phys. Rev. E **65**(4), 041107 (2002)

45. Golub, G., van Loan, C.: Matrix Computations, 3rd edn. Johns Hopkins University Press, London (1996)
46. Cooley, J.W., Tukey, J.W.: Math. Comput. **19**, 297 (1965)
47. Wu, Z., et al.: PNAS **104**(38), 14889–14894 (2007)
48. Nagarajan, R., Kavasseri, R.G.: Chaos Solitons Fractals **26**(3), 777–784 (2005)
49. Nagarajan, R., Kavasseri, R.G.: Physica A **354**, 182–198 (2005)
50. Hajian, S., Movahed, M. Sadegh: Physica A **389**, 4942–4957 (2010)
51. Lieberman, M.A., Lichtenberg, A.J.: Principles of Plasma Discharges and Materials Processing. Wiley, New York (1994)
52. Chen, F.F.: Introduction to Plasma Physics. Plenum Press, New York (1974)
53. Cap, F.F.: Handbook on Plasma Instabilities. Academic Press, New York (1976)
54. Nishikawa, K., Wakatani, M.: Plasma Physics, 3th edn. Springer, Berlin (1999)
55. Risken, H.: The Fokker-Planck Equation. Springer, Berlin (1984)
56. Van Kampen, N.G.: Stochastic Processes in Physics and Chemistry. North Holland, Amsterdam (1981)
57. Gardiner, C.W.: Handbook of Stochastic Methods. Springer, Berlin (1983)
58. Ḧanggi, P., Thomas, H.: Phys. Rep. **88**, 207 (1982)
59. Renner, C., Peinke, J., Friedrich, R.: JFM **433**, 383 (2001)
60. Friedrich, R., Zeller, J., Peinke, J.: Europhys. Lett. **41**, 153 (1998)
61. Colistete, R. Jr., Fabris, J.C., Goŋcalves, S.V.B., de Souza, P.E.: Int. J. Mod. Phys. D **13**(4), 669 (2004)
62. Medvedev, S.Y.: Radiophys. Quantum Electron. **20**(8), 863–865 (1977)
63. Dynkin, E.B.: J. Funct. Anal. **55**(3), 344–376 (1984)
64. Primak, S., Lyandres, V., Kontorovich, V.: Phys. Rev. E **63**(6), 061103 (2001)
65. van Milligen, B.P., Sánchez, R., Carreras, B.A., Lynch, V.E., LaBombard, B., Pedrosa, M.A., Hidalgo, C., Gonçalves, B., Balbin, R.: Phys. Plasmas **12**, 052507 (2005)
66. Sattin, F.: arXiv:0903.2189
67. Renner, C., Peinke, J., Friedrich, R.: Physica A **298**(3–4), 499–520 (2001). arXiv:cond-mat/0102494v2 (2000)
68. Waechter, M., Riess, F., Schimmel, Th., Wendt, U., Peinke, J.: Eur. Phys. J. B **41**(2), 259 (2004)
69. Hurst, H.E., Black, R.P., Simaika, Y.M.: Long-Term Storage: An Experimental Study. Constable, London (1965)
70. Eke, A., Herman, P., Kocsis, L., Kozak, L.R.: Physiol. Meas. **23**(1), R1 (2002)
71. Koscielny-Bunde, E., Roman, H.E., Bunde, A., Havlin, S., Schellnhuber, H.J.: Philos. Mag. B **77**(5), 1331 (1998)
72. Koscielny-Bunde, E., Bunde, A., Havlin, S., Roman, H.E., Goldreich, Y., Schellnhuber, H.J.: Phys. Rev. Lett. **81**(3), 729 (1998)
73. Benzi, R., Biferale, L., Ciliberto, S., Struglia, M.V., Tripiccione, R.: Physica D **96**(1–4), 162 (1996)
74. Bershadskii, A., Sreenivasan, K.R.: Phys. Lett. A **319**(1–2), 21 (2003)
75. Kolmogorov, A.N.: Dokl. Akad. Nauk SSSR **31**, 538 (1941)
76. Anselmet, F., Gagne, Y., Hopifinger, E.L., Antonia, R.A.: J. Fluid Mech. **140**, 63 (1984)
77. Benzi, R., Paladin, G., Parisi, G., Vulpiani, A.: J. Phys. A **17**, 3521 (1984)
78. Meneveau, C., Sreenivasan, K.R.: Nucl. Phys. B, Proc. Suppl. **2**, 49 (1987)
79. Benzi, R., Ciliberto, S., Tripiccione, R., Baudet, C., Massaioli, F., Succi, S.: Phys. Rev. E **48**, R29–R32 (1993)
80. Ghasemi, F., Kaviani, K., Sahimi, M., Rahimi Tabar, M.R., Taghavi, F., Sadeghi, S., Bijani, G.: Comput. Sci. Eng. **8**(2), 54 (2006)
81. Gentle, K.W.: Rev. Mod. Phys. **67**(4), 809 (1995)
82. Krommes, J.A.: Phys. Rep. **360**(1–4), 1 (2002)
83. Oberman, C.R., Williams, E.A.: In: Galeev, A.A., Sudan, R.N. (eds.) Basic Plasma Physics, vol. 1. North-Holland, Amsterdam (1983)
84. Taylor, E.C., Comisar, G.G.: Phys. Rev. **132**(6), 2379 (1963)
85. Hazeltine, R.D., Mahajan, S.M.: Phys. Plasmas **11**(12), 5430 (2004)
86. Schappe, R.S., Walker, T., Anderson, L.W., Lin, C.C.: Phys. Rev. Lett. **76**, 4328 (1996)
87. Bernshtam, V.A., Ralchenko, Yu.V., Maron, Y.: J. Phys. B, At. Mol. Opt. Phys. **33**(22), 5025–5032 (2000)
88. Ichimaru, S.: Statistical Plasma Physics, Condensed Plasmas, vol. II (2004). Westview Press